Chapter 15
Characterization and Removal of a Disfiguring Oxalate Crust on a Large Altarpiece by Hans Memling

Lizet Klaassen, Geert van der Snickt, Stijn Legrand, Catherine Higgitt, Marika Spring, Frederik Vanmeert, Francesca Rosi, Brunetto Giovanni Brunetti, Marie Postec, and Koen Janssens

Abstract During the conservation treatment of Memling's *Christ with Singing and Music-making Angels*, three panel paintings that are among the most monumental works in early Netherlandish art, the conservators came across insoluble surface layers containing calcium oxalates. A very thin and irregular layer of this type, hardly visible to the naked eye, was spread across the surface of all three panels. A much thicker layer forming an opaque and highly disfiguring crust that obscured the composition (Figs. 15.1 and 15.7) was locally present on areas of dark copper-containing paint, where multiple layers of old discolored coatings and accretions remained in place before the most recent cleaning.

This article describes the application of a wide range of analytical techniques in order to fully understand the stratigraphy and composition of the crusts on the Memling paintings. FTIR spectroscopy in transmission and reflection mode, micro-ATR-FTIR imaging and macro-rFTIR scanning, SEM-EDX, mobile XRD,

L. Klaassen (✉)
Royal Museum of Fine Arts Antwerp, Antwerp, Belgium
e-mail: lizet.klaassen@kmska.be

G. van der Snickt
Department of Chemistry – AXES group, University of Antwerp, Antwerp, Belgium

Conservation Studies, University of Antwerp, Antwerp, Belgium

S. Legrand · F. Vanmeert · K. Janssens
Department of Chemistry – AXES group, University of Antwerp, Antwerp, Belgium

C. Higgitt · M. Spring
The National Gallery, London, UK

F. Rosi · B. G. Brunetti
Istituto CNR di Scienze e Tecnologie Molecolari (CNR-ISTM), Perugia, Italy

Centro di Eccellenza SMAArt, Università degli Studi di Perugia, Perugia, Italy

M. Postec
Independent Painting Conservator, Brussels, Belgium

F. Casadio et al. (eds.), *Metal Soaps in Art*, Cultural Heritage Science,
https://doi.org/10.1007/978-3-319-90617-1_15

and SR-μXRD showed that the crusts contained two related Ca-based oxalate salts, whewellite and weddellite, and were separated from the original paint surface by varnish, indicating that they did not originate from degradation of the original paint but from a combination of microbial action and a thick accumulation of dirt. Supported by the results from these different analytical techniques, which when used together proved to be very effective in providing complementary information that addressed this specific conservation problem, and aided by the presence of the intermediate varnish layer(s), the conservators were able to remove most of the crusts with spectacular results.

Keywords Memling · Christ with Singing and Music-making Angels · MA-rFTIR · ATR-FTIR · SR-μXRD · SEM-EDX · KMSKA · Oxalate · Whewellite · Weddellite

15.1 Introduction

One of the highlights in the collection of the Royal Museum of Fine Arts Antwerp is three large panel paintings entitled *Christ with Singing and Music-making Angels*, attributed to Hans Memling and assistants (Fig. 15.1). This paper deals with its

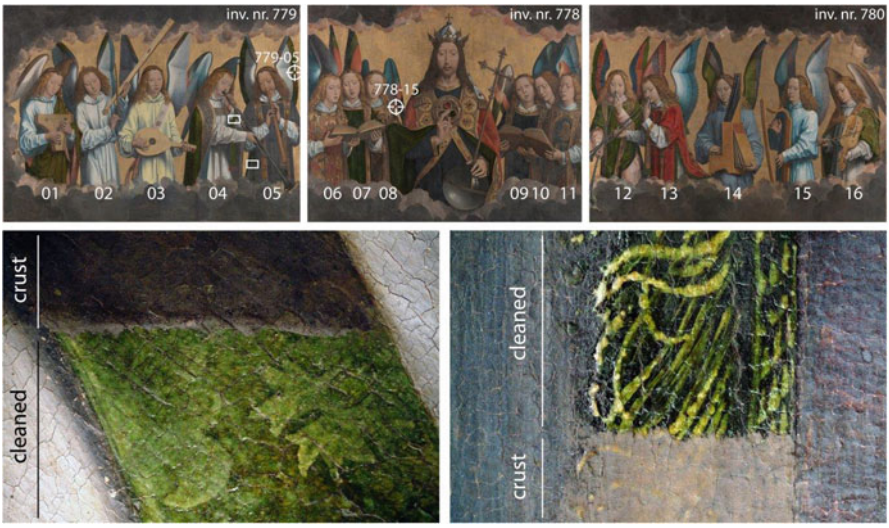

Fig. 15.1 Top row: *Christ with Singing and Music-making Angels* attributed to Hans Memling and assistants. Collection of the Royal Museum of Fine Arts Antwerp (KMSKA), with numbering of the angels and indication of sample locations (crosshair). The white rectangles indicate the location of the details shown in the bottom row. Bottom row: two macrophotographs showing two areas on panel 779 where oxalate crusts on green paint had been partly removed. Photos top row: KMSKA © Photo Rik Klein Gotink. Photos bottom row: KMSKA © Arcobaleno, Adri Verburg

extraordinary conservation treatment, which took from 2001 until 2017 and involved a team of conservators and scientists.

15.2 Memling's Retablo Major

Christ with Singing and Music-making Angels consists of three large panel paintings: the central panel measures 170 × 213 cm, and the two side panels are 170 × 231 cm each. The panels are attributed to Hans Memling and assistants and were made at the end of the fifteenth century, so late in Memling's career (Fransen 2018). Despite their sizeable dimensions, the panels are only a fragment of the original work of art. Originally, they formed the upper row of what must have been a very large polyptych, created for the high altar of the monastery of Santa Maria la Real in Nájera, Spain. The panels were described in 1795 by the Spanish writer Gaspard David Jovellanos who saw them, together with a large *Assumption of the Virgin*, two apostles, and the Saints Benedictus, Prudentius, Vitalis, and Agricola, on his visit to Nájera. According to Jovellanos, all of the artworks were by the same artist and belonged to the same altarpiece. Jovellanos saw the different parts in various places in the Monastery, the altarpiece having already been dismantled by 1795, but the *Assumption of the Virgin* was probably originally placed below Christ and flanked by the saints (Vandenbroeck 1985; Borchert 1993; De Vos 1994).

Although the Antwerp panels are undoubtedly among the most monumental works in early Netherlandish painting, not much is known about their history. As indicated above, the polyptych had already been dismantled by 1795, and when the panels were rediscovered around 1880 by Spanish art dealers, the central panel, *Christ with Singing Angels,* was placed above an altar, and the side panels, *Music-making Angels*, formed part of an organ decoration. After a stay of almost 400 years in Nájera, in 1886 the panels were sold to art dealers and finally bought by the Royal Museum of Fine Arts Antwerp in 1895.

The different retouching campaigns visible on the paint surface and the cradles on the back, probably attached in the 1950s or 1960s, indicated that there must have been several interventions in the past. However, there is very little documentation on the conservation history of the panels. Before they entered the art dealer circuit, they were brought to Madrid and "cleaned."[1] In the museum archives just a few, very short notes were found describing only minor interventions executed after their purchase.[2]

[1] "Llegó a Madrid, donde, tras su limpieza, se intentó que lo comprara la Reina Maria Christina," (Gómara 2013). Many thanks to Sara Mateu for providing the article.

[2] Flaking paint was noted in February and May 1901, in different areas. It was mentioned that the panels were covered by a layer of dust that adhered to the surface and diminished the brightness of the colors. Consolidation and surface cleaning with bread crumbs was proposed, but the charge made for the work was only for consolidation.
In 1952, 1977, and 1980, the panels occur in lists among other paintings that were treated, but

15.3 The Need for Intervention in 2001

The poor condition of the paintings was the impetus for the extensive conservation treatment that began in 2001. By that time there was severe flaking of the paint layers, the cradles were blocked, and the surface was extremely dirty. The consolidation of the paint layers and the unblocking of the cradles were the first steps of the treatment, and both could be executed without major problems. The cleaning, however, turned out to be problematic and took years to complete. Yellowed varnishes, discolored retouching, and layers of dirt subdued the bright colors and greatly reduced the legibility and the three-dimensionality of the composition. It was only through technical imaging, including infrared photography, infrared reflectography (IRR),[3] and X-ray radiography (XRR),[4] that the conservators became aware that underneath some of the plain, flat brown areas, decorative details, as well as modelling of the volume and folds in the draperies were present.

Cleaning tests showed that underneath the uppermost soluble varnish layers, a grey-brown opaque crust was present in the darkest, most obscured areas, in particular over the copper-containing blue and green paint and the grey clouds surrounding the figures, which also contain a copper-based pigment in the form of azurite.[5]

Unfortunately, this crust turned out to be highly insoluble in the extensive range of solvents and cleaning systems that were tested. It reacted to the cleaning tests by blanching but appeared impossible to dissolve. To gain more insight into its composition and with the hope of finding a safe method to remove it, scrapings of it were first analyzed by transmission FTIR microscopy and SEM-EDX. Further non-invasive investigations and detailed analysis of samples mounted as cross sections were also undertaken subsequently, in order to gain a more precise understanding of the chemical composition of the crusts, their location in the layer structure, and their distribution across the paint surface.

---

details were not specified. Although nothing is mentioned about the cradles, judging from their appearance, it is thought that they were attached in the 1950s or 1960s when the panels were already in the museum. In addition, a synthetic varnish (isobutyl acrylate) was found on the surface which must also have been applied in the museum.

[3]Infrared imaging was carried out twice: at the beginning of the project by Adri Verburg, using a phase I scanning back (4 × 5 inch) with spectral range 1000–1100 nm, and during the project by Claudia Daffara and Mattia Patti, using a multispectral scanner, spatial resolution 4 pt./mm (250 micron), InGaAs with spectral range 800–1700 nm, C.N.R.–I.N.O.A (Istituto Nazionale di Ottica Applicata).

[4]X-radiography was undertaken by Guido van de Voorde, Royal Institute for Cultural Heritage, Parc du Cinquantenaire 1, B-1000 Brussels.

[5]SEM-EDX detected copper in the blue and green paints, suggesting the use of azurite and a copper-containing green pigment (most probably originally verdigris). The grey paint layer depicting the clouds consists mainly of a mixture of lead white and a black pigment (probably a carbon-based black), mixed with a little azurite, identified by SEM-EDX and FTIR microscopy.

15.4 Experimental

Transmission Fourier transform infrared (FTIR) microscopy (mid-IR range) spectra were acquired using a Nicolet 710 Series FTIR spectrometer with a NicPlan infrared microscope, fitted with a mercury-cadmium-telluride (MCT) type A detector (cooled with liquid nitrogen). Small subsamples of the scrapings of the crusts were placed between the windows of a Spectra-Tech micro-compression diamond cell for analysis. Measurements were made in transmission mode over the range 4000–650 cm^{-1}, using a Spectra-Tech Reflachromat Cassegrain ×15 objective. One hundred twenty-eight or 256 scans were made at a resolution of 4 cm^{-1} with Happ-Genzel apodization. Both spectrometer and microscope were purged with water- and CO_2-free air.

Mobile reflection mid-infrared (reflection mid-FTIR) spectrometry point measurements were performed by means of a portable JASCO VIR 9500 spectrophotometer, made up of a Midac Illuminator IR radiation source, a Michelson interferometer, and a liquid nitrogen-cooled MCT detector. The probe was a 4 mm bifurcated cable containing 19 chalcogenide glass fibers allowing collection of spectra in the range 4000–900 cm^{-1} at a resolution of 4 cm^{-1}. The noncontact probe was kept perpendicular to the painting surface (0°/0° geometry) at a distance of about 3 mm. The total reflectance was collected over 400 scans using the spectrum from an aluminum mirror plate for background correction. The reflectance spectra (R) were converted to pseudo-absorbance (A' = log(1/R)).

The instrument used for the macroscopic FTIR scanning measurements in reflection mode (MA-rFTIR scanner) was a Bruker Alpha FTIR spectrometer, equipped with a frontal reflection module (20°/20° geometry) and a coaxial visual camera (Legrand et al. 2014). The spectrometer incorporates a globar IR source, Michelson interferometer, and a deuterated triglycine sulfate (DTGS) detector. Spectra acquisition and storage were carried out using the Bruker OPUS 6.0 software package. Before each scan a spectral background was recorded over 30 min by placing a gold-coated mirror in front of the reflection module. During scanning mode, spectra were recorded for 3 s on each point at a resolution of 4 cm^{-1} over the range 7500–375 cm^{-1}. For scanning purposes, the spectrometer was mounted on a motorized X (10 cm), Y (25 cm), and Z (10 cm) motor stage setup (Newport Corporation, Irvine, CA, USA). The X and Y stages are used during scanning, while the Z stage helps to bring the setup in focus (2 mm spot) prior to the scan. The processing of the hyperspectral datasets was performed by self-written routines using the data analysis software package IDL 8.3. For most chemical distributions and spectra, the recorded reflectance was converted to pseudo-absorbance. The resulting FTIR maps have a lateral resolution in the mm range.

For mobile X-ray diffraction (MXRD) measurements combined with XRF, a 30 W air-cooled iMOXS-MFR (IFG, Adlershof, Berlin, Germany) X-ray tube was used with a voltage of 40 kV and a current of 700 μA. The source is equipped with a polycapillary semi-lens providing a 4 mm (3.8–4.4 mm) diameter parallel X-ray beam (total exit divergence of 0.25° or 4.36 mrad). The copper anode

provides, through a 0.1 mm beryllium window, polychromatic X-rays necessary for XRF measurements. The source is equipped with a 15 μm Ni filter to strongly attenuate the Cu K_β-line and avoid the presence of secondary diffraction peaks. XRD is therefore performed with the usual monochromatic radiation (Cu-K_α; E = 8.047 keV (= 0.154 nm)). Diffractograms are collected in reflection mode using an incident angle ω of 10° to the specimen surface allowing 2θ values larger than 10° to be reached. Fine-grain alumina samples were used for the calibration. The relatively prolonged acquisition times, amounting up to 30 min, limited the number of measurements. The FIT 2D software[6] was used to transform the two-dimensional diffraction images into 2θ spectra. Based on the latter and a database of X-ray powder diffraction patterns, the EVA[7] and XRDUA[8] software were used to determine the crystalline phases that were present. The technical features and analytical performance of this instrument are discussed elsewhere (Gianoncelli et al. 2008).

At the University of Antwerp, embedded paint cross sections were analyzed by means of a Jeol 6300 electron microprobe system equipped with an energy dispersive Si (Li) X-ray detector (SEM-EDX) (Princeton Gamma Tech). Elemental distribution maps were collected from the surface of paint cross sections at 20 kV, a magnification of 500×, a beam current of 1 nA, and a recording time of 3600 s.

The elemental analysis and mapping that was carried out at the National Gallery on paint cross sections and scrapings was done using a Carl Zeiss EVO® MA10 variable pressure scanning electron microscope (SEM) coupled to an Oxford Instrument X-Max 80 mm^2 energy dispersive X-ray spectrometer (EDX), using INCA 350 software. The operating parameters were 20 kV, 200 pA beam current, and 30 Pa chamber pressure (the minimum necessary to limit charging) with air as the chamber gas. Optical microscopy was carried out using a Leica DM4000 M microscope and a Zeiss AxioCam HRc camera for recording images. A filter system A (BP 340–380 nm, dichromatic mirror: 300 nm, suppression filter: LP 425 nm) was used for UV excitation.

Attenuated total reflection Fourier transform infrared (ATR-FTIR) microspectroscopic imaging spectra were acquired from embedded cross sections by using a Bruker Tensor 27 FTIR spectrometer connected to a Hyperion 3000 Series microscope, fitted with a 64 × 64 (4096 pixels) FPA detector (range = 4500–900 cm^{-1}), cooled with liquid nitrogen. The microscope was fitted with a CCD camera, X-Y stage (adjustment accuracy of 0.1 μm), and a dedicated ATR objective (20× magnification). The ATR had a germanium crystal with a tip size of 250 μm. Both spectrometer and microscope were purged with water- and CO_2-free air. One hundred twenty-eight scans were collected at a resolution of 4 cm^{-1}. The 64 × 64 pixel focal plane array collects image data from a 32 × 32 μm square. An effective (diffraction limited) lateral resolution of 3–5 μm is achieved.

[6] http://www.esrf.eu/computing/scientific/FIT2D/. Accessed February 2017.

[7] http://www.bruker-axs.de/eva.html. Accessed February 2017.

[8] http://xrdua.ua.ac.be/. Accessed February 2017.

Combined synchrotron radiation-based micro X-ray fluorescence and micro X-ray diffraction (SR μ-XRF/μ-XRD) imaging experiments were performed at the microprobe station of the P06 Hard X-ray Micro/Nano-Probe beamline (PETRA III, DESY, Germany). A photon energy of 21 keV was selected by means of a Si(111) double crystal monochromator. The beam was focused to 0.4 × 0.4 μm^2 (hor. × vert.) employing a Kirkpatrick-Baez mirror optic. Fluorescence radiation was recorded by a Vortex-EM silicon drift detector placed perpendicular to the incident X-ray beam. Simultaneously diffraction signals were recorded in transmission geometry using a Pilatus 300 K area detector at a distance of approximately 15 cm behind the sample. Initial calibration of the diffraction setup was performed using a LaB_6 reference sample. The software package PyMCA was used for spectral fitting of the fluorescence data (Solé et al. 2007), while whole pattern fitting of the diffraction data was performed using XRDUA (De Nolf and Janssens 2010). This software package provides several methods for obtaining crystalline-specific distributions from a large number of diffraction patterns typically obtained in μ-XRPD imaging experiments (De Nolf et al. 2014).

15.5 Analytical Results

15.5.1 Analysis of Scrapings of the Crust

Since rapid identification of the crusts was vital for the continuation of the conservation treatment, a number of samples in the form of scrapings were taken and analyzed after local removal of the upper varnish layers. These were collected from each panel, concentrating in particular on the crusts on the blue and green paint and on the grey clouds. The resulting powders were analyzed using FTIR microscopy in transmission mode and SEM-EDX at the National Gallery, London. All of the samples of the crusts had a similar composition, consisting essentially of calcium oxalate (bands at c.1650, 1327, and 783 cm^{-1}), with some calcium carbonate (c.1414, 875, and 712 cm^{-1}) and calcium sulfate (c.3401, 1120, and 671 cm^{-1}). In addition, when interpreted with the SEM-EDX results, the broad band at c.1090 (together with the doublet at c.800/780 cm^{-1}) indicates the presence of various silicates, and the band at c.1041 cm^{-1} shows the presence of calcium phosphate (and/or silicates such as phyllosilicates with bands at c.1040 and 915 cm^{-1}) (Farmer 1974). This composition suggests that the layer most probably resulted from an accumulation of dirt on the surface.[9]

[9]C. Higgitt and M. Spring, *Preliminary EDX and FTIR microscopic examination of samples*, National Galley, unpublished research report. For comparable spectra see the appendix in Higgitt and White (2005). For the chemical composition of dirt, see Van Grieken et al. (2000).

15.5.2 Non-invasive Analysis

In cooperation with the University of Antwerp and as part of a MOLAB campaign (Miliani et al. 2010),[10] the crusts were further investigated using mobile analytical equipment (Van der Snickt et al. 2011). The noncontact and non-invasive approach typical of MOLAB allowed a large number of measurements to be performed all over the vast paint surface of all three panels. In this way it was possible to assess the extent to which the local data obtained from a few scrapings was representative of the rest of the large surface.

Monico et al. demonstrated the usefulness and sensitivity of reflection mid-FTIR spectroscopy for the non-invasive identification of various oxalate salts on the surface of polychrome works of art (Monico et al. 2013). Interestingly, MOLAB reflectance FTIR point measurements, performed with the same instrument that was employed in that study, indicated the presence of oxalates across the entire paint surface. As exemplified by the spectrum in Fig. 15.2, characteristic calcium oxalate

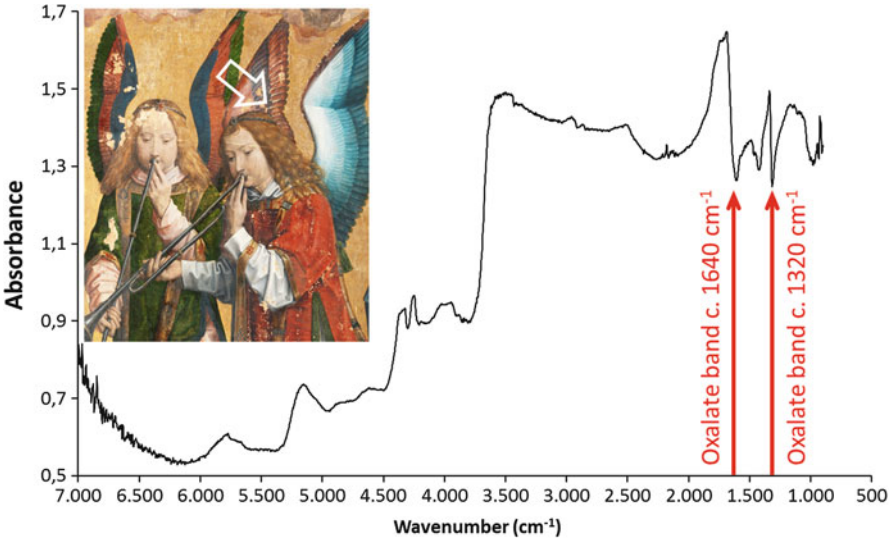

Fig. 15.2 Reflection mid-FTIR spectrum recorded on a reddish feather of angel 13 in an area where no crusts were observed. Insert: a white arrow indicates the exact spot where the spectrum was collected. Characteristic calcium oxalate bands around 1320 and 1640 cm^{-1} are indicated by red arrows

[10]MOLAB is a mobile laboratory composed of a unique collection of portable equipment which is available to cultural heritage researchers across Europe, including art historians, conservators, and conservation scientists. The MOLAB analyses presented here were funded under the EU CHARISMA project (FP7, grant no. 228330). MOLAB can currently be accessed through the Horizon 2020 IPERION project (www.iperionch.eu, Grant No. 654028).

bands at around 1320 and 1640 cm^{-1} were observed in all FTIR measurements, including those collected in areas where no crusts were visible to the naked eye. At the end of the campaign, it was evident that there was an oxalate-containing layer distributed across the whole paint surface of all three panels but so thin that it was hardly visible to the naked eye.

The numerous non-invasive reflectance FTIR measurements on the thicker crust present above areas of dark copper-containing paint also revealed exclusively calcium oxalates, with no evidence of the formation of the analogous compounds with copper, in agreement with the transmission FTIR analyses of the scrapings. Measurements performed on the crusts with the mobile X-ray diffraction (XRD) instrument from the C2RMF (Gianoncelli et al. 2008) confirmed the presence of two related Ca-based oxalate salts: whewellite and weddellite.[11]

15.5.3 Analysis of Paint Cross Sections

While the characterization of scrapings and non-invasive analysis of the paintings allowed identification of the surface materials, more detailed information about the layer structure of the paint and coatings was considered essential in order to assess the feasibility of removal of the crusts. The extensive non-invasive analysis guided the selection of sample locations and reduced the number of samples that were needed. The samples were taken both from areas where the thick, opaque crusts were evident and from areas where the oxalate-containing layer was hardly visible to the naked eye. The main objective was to compare these areas through the examination of paint cross sections and to gain insight into the location of the oxalate-containing layers within the overall layer structure.

Figure 15.3 shows the stratigraphy of the cross section prepared from a sample taken from the crust on top of the green feathers of the wing of angel 5 on panel 779. Figures 15.4 and 15.5 show the results of SEM-EDX analysis and micro-ATR-FTIR imaging of this sample. ATR-FTIR microspectroscopic imaging (Fig. 15.5) is a technique that was not available at the time of the first FTIR analyses on scrapings but since its introduction has proved very valuable for chemical imaging at high resolution (up to about 3 μm is achievable) directly on cross sections. It is especially suited to the characterization and location of oxalate-containing accretions.

At the bottom of the cross section are the ground layers on top of which are a thin brownish mordant and a layer of gold leaf (all layers labelled together as "1" in Figs. 15.3, 15.4, and 15.5). The ground in this sample consists of a first thin gypsum-rich layer followed by a thick chalk-rich layer. The gilded background

[11] In principle, whewellite and weddellite can also be distinguished on the basis of their FTIR spectra (although there is some disagreement in the literature about precise band positions), but in practice this is difficult, particularly when the salts are present in mixtures or in combinations with other compounds, see, for example, Garty et al. (2002), Conti et al. (2010), and Leroy (2016).

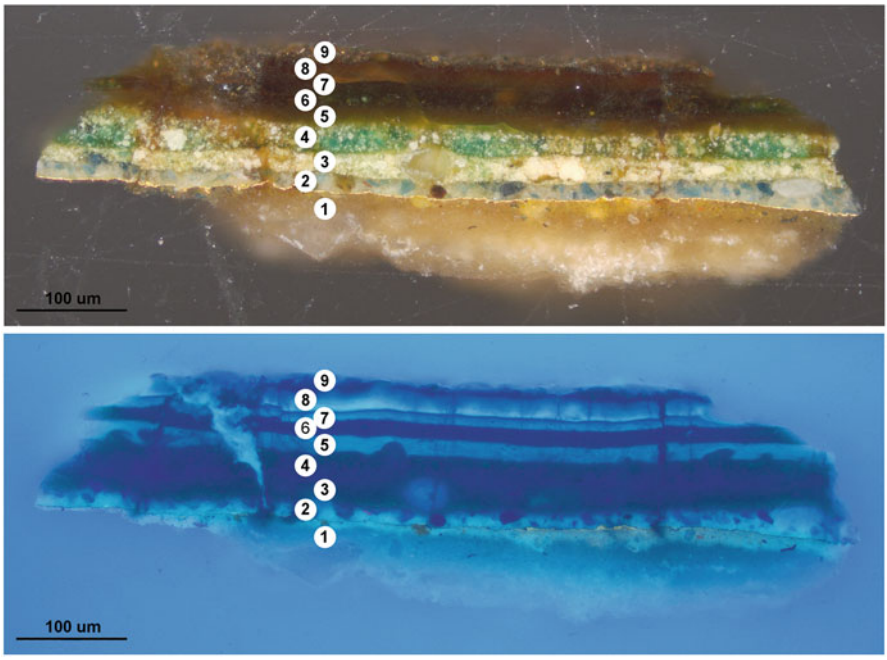

Fig. 15.3 Top: optical microscopy (OM) image of the cross section prepared from sample 779-05, removed from the green wing of angel 5, taken with visible illumination, and showing the sample stratigraphy. Bottom: photomicrograph of the same cross section taken under UV illumination

extends beneath the paint in this area. The next layer (labelled 2) contains a mixture of lead white and azurite and appears to correspond to the paint used to create the inner part of the wing. Over the blue paint is a light yellow-green paint (labelled 3) composed of a copper-containing pigment (probably verdigris or a related copper salt of an organic acid), lead white and lead-tin yellow (type I). This is covered with a more deeply colored green paint (labelled 4), containing a similar mixture to layer 3 but with rather less lead white and lead-tin yellow. Detailed examination of a series of FTIR spectra extracted from the ATR-FTIR imaging data confirmed that the copper-containing pigment in this layer is some form of (basic) copper acetate and revealed the presence of copper carboxylates (strong asymmetric carboxylate stretch at 1586 cm^{-1}), presumably from reaction of the pigment with the oil binder, and copper oxalates. Directly over the green paint is a very brown oil-resin varnish layer (labelled 5), which also contains some copper oxalate, suggesting migration of copper from the paint layer below. Over this varnish is a layer with a greenish color (labelled 6), which can be seen in the EDX maps to contain copper (both dispersed throughout the layer and in discrete copper-rich particles) and a little calcium. ATR-FTIR indicates that at least some of the copper in this layer is present in the form of copper carboxylates and oxalates. Since it lies over varnish, it is not completely

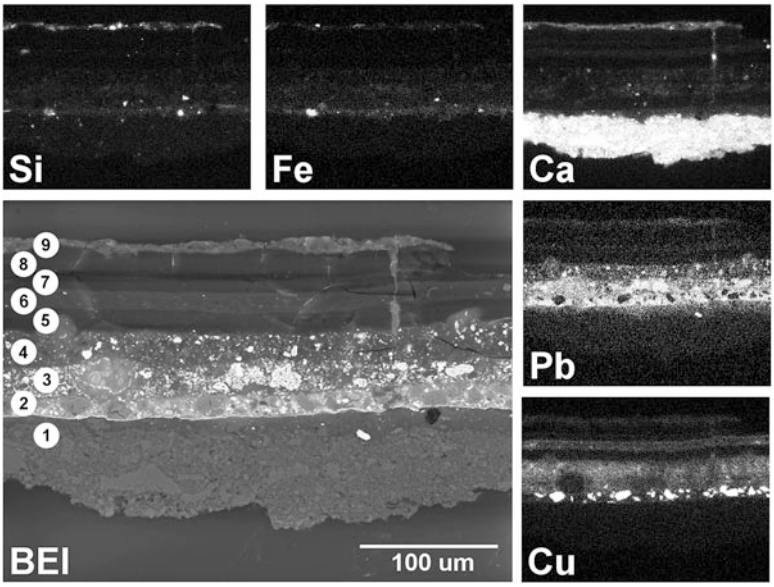

Fig. 15.4 SEM-EDX measurements on sample 779-05 taken from the green wing of angel 5. Bottom left: backscattered electron image (BEI) showing the sample stratigraphy. Top: elemental distribution maps of silicon (crust and mordant) and iron (crust and mordant). Right, top to bottom: elemental distribution maps of calcium (crust and ground, plus smaller quantities in the paint layers and the intermediate copper-containing layer), lead (paint layers), and copper (paint layers and intermediate layer between varnish layers)

clear whether this copper-containing layer is overpaint or an original glaze,[12] but it is covered by at least one, or possibly two, further oil-resin varnish layers (labelled 7 and 8). Copper oxalates were detected in the lower part of the varnish on top of the intermediate green layer (corresponding to layer 7) but not further up within the stratigraphy.[13] The calcium EDX map (Fig. 15.4) shows a thick calcium-rich layer (labelled 9) at the very top of the stratigraphy, corresponding to the calcium oxalate-containing crust, as can be seen in the ATR-FTIR imaging results (Fig. 15.5). The

[12] Although the conservators were of the opinion that the copper-containing paint on top of the varnish layer was probably overpaint, it was left on the surface during cleaning as no certain proof for this could be found in the cross sections or on the surface of the paintings. It was not present as a continuous layer but more as local spots.

[13] The location of the copper oxalates suggests that some degree of migration of copper ions into adjacent layers has occurred but not all the way up into the surface crust. These results clarify why only calcium oxalates were detected at the surface of the paintings in the scrapings and using the MOLAB non-invasive reflectance FTIR equipment. It should be noted that calcium oxalates may also be present in those layers containing copper oxalates, but this cannot be confirmed because of the overlap of the spectral bands and the 900 cm^{-1} cutoff for the micro-ATR-FTIR imaging equipment.

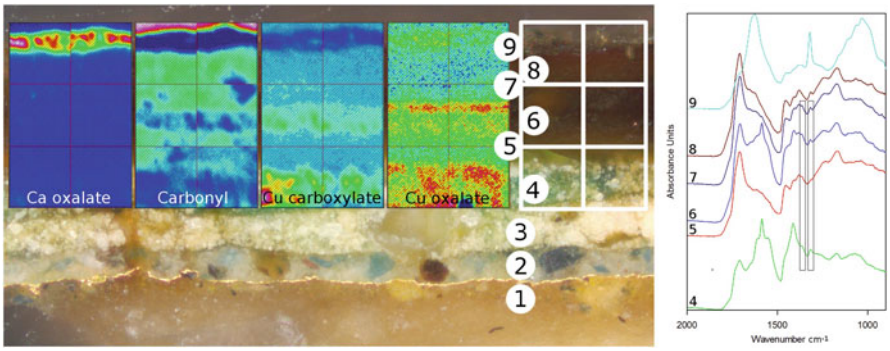

Fig. 15.5 Left: series of ATR-FTIR images produced by integration of IR spectral bands revealing the location of different materials within sample 779-05 taken from the green wing of angel 5. From left to right: the image produced by integration of the band between 1333 and 1302 cm^{-1} shows the distribution of calcium oxalates; between 1741 and 1674 cm^{-1} shows the distribution of carbonyl groups associated primarily with the oil-resin varnish layers, the paint, and the polyester mounting resin; between 1599 and 1564 cm^{-1} shows the distribution of copper carboxylates (and the green copper-containing pigment(s)); and between 1371 and 1345 cm^{-1} shows the distribution of copper oxalates. The scan window is 64 μm wide and 96 μm tall, i.e., 2 × 3 32 μm squares. Right: series of FTIR spectra from the different layers extracted from the ATR-FTIR imaging data. (9) Surface crust (calcium oxalate at c.1650 and 1321 cm^{-1}), (8) varnish layer directly below crust (oil-resin varnish at c.1733, 1711, 1435, 1414, 1318, 1254, and 1166 cm^{-1}), (7) varnish layer directly above copper-containing intermediate layer (possibly same layer as layer 8), (6) copper-containing intermediate layer (strong asymmetric carboxylate stretch at 1587 cm^{-1}), (5) varnish layer directly above paint (as above), and (4) upper green paint layer (copper-based pigment and copper carboxylates at c.1615, 1586, 1546, and 1414 cm^{-1}). Copper oxalates can be detected in layers 4–7 only (determined by the presence of the highlighted bands at c.1364 and 1319 cm^{-1})

elemental distribution maps reveal the heterogeneous nature of the crust which contains, in addition to calcium, distinct particles rich in silicon and iron.

Another sample was taken from the red lake-containing glaze in the feathers of the wing of angel 8 on panel 778. This was an area where the oxalate-containing surface layer was hardly visible to the naked eye. The sample was imaged using synchrotron radiation-based μ-XRF/μ-XRD mapping, and a number of the resulting chemical images are shown in Fig. 15.6. The XRD mapping shows a very thin layer (less than 1 μm) containing weddellite at the very top of the stratigraphy. Compared to the oxalate layers in the cross section that include the thick crust (see Figs. 15.3, 15.4, 15.5), this layer is much thinner, which explains why the oxalate deposits are hardly visible to the naked eye in this area. The oxalate layer might seem to be directly on top of the red lake-containing paint, but in fact – although this is not very clear in Fig. 15.6 – other chemical images of this cross section show that the weddellite-containing layer is separated from the original paint by an organic layer, presumably varnish (Janssens et al. 2016). At the very bottom of the cross section, the preparation layers are visible: the ground appears to consist of two layers, a layer rich in chalk applied over a layer rich in gypsum. The technique allowed the detected

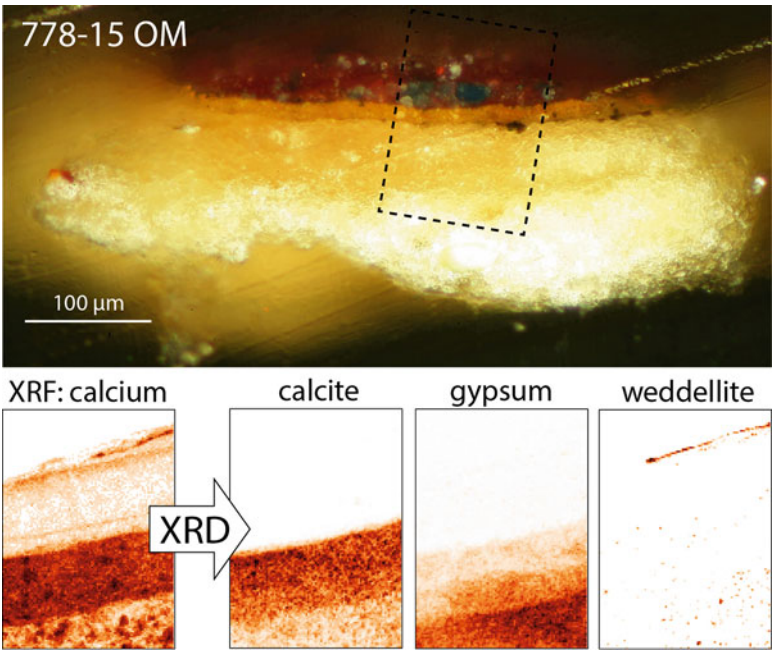

Fig. 15.6 Top: micrograph of sample 778–15 taken from the feathers of angel 8. The black rectangle indicates the area that was chemically imaged. Below: chemical images obtained by means of synchrotron radiation-based μ-XRF/μ-XRD. Bottom left: μ-XRF map of calcium collected in reflection mode. Bottom right: corresponding μ-XRD maps (transmission mode) of three calcium species: calcite, gypsum, and weddellite

calcium fluorescence signal to be resolved into four separate species: gypsum and calcite in the ground, hydroxylapatite on top of the ground (not shown), and a thin layer of weddellite at the top.

15.6 Discussion

The formation of metal oxalates, and particularly oxalate-rich surface layers, is commonly observed for a wide range of artworks including stone and bronze sculpture, wall paintings, and stained glass (Zoppi et al. 2010). Such oxalate-rich crusts, which are essentially inorganic in composition and highly insoluble, induce scatter and can be highly disfiguring. As oxalate and other salts form on surfaces, colored components of dirt (e.g., carbon-containing particles) can also become trapped within the crust, as observed on building stone (Potgieter-Vermaak et al. 2005). In recent literature, oxalate-containing layers on the surface of easel paintings

are being reported with increasing frequency.[14] Although on easel paintings these layers are generally thin, their scattering effect gives an unsaturated appearance and can be optically very disturbing, especially in the dark areas. Nevertheless, during conservation treatments, these oxalate-containing layers are often left essentially undisturbed on the surface as their insolubility and strong adhesion to underlying layers make it impossible to remove them selectively.

The origin and formation of oxalate salts is complex and not fully understood. A number of different mechanisms may be involved depending on the exact materials and environment, but in general, oxalate salts form when oxalic acid reacts with metal ions. In paintings, the metal cations may originate from the paint layers (e.g., pigments or driers (Van der Snickt et al. 2012)), from the ground/substrate, or from particulate matter such as dirt deposited on the paint surface, but the source of the oxalic acid is still a subject of debate (Spring and Higgitt 2006). Microbiological activity and some form of extreme chemical deterioration of organic substances, either within the paint (e.g., the binder) or on the paint surface (e.g., protective or other coatings), have both been suggested in the literature (Mendes et al. 2008; Zoppi et al. 2010). It appears that either or both of these processes can be a source, but it is also clear that oxalate formation can occur even in the absence of an organic material (or where only small amounts are present).

In the case of Memling's *Christ with Singing and Music-making Angels,* a calcium oxalate-containing layer was found over the entire surface of the paintings, but in most areas, over light colors, this layer was so thin (less than 1 μm) that it was hardly visible to the naked eye. The oxalate-containing crusts on the darkest areas of the painting, however, were exceptionally thick, with an opaque grey-brown appearance, and highly disfiguring. Such crusts were present primarily over dark copper-containing paints, including the green garments painted with verdigris, and to a lesser extent over the azurite-rich garments and the grey clouds, which also contain a little azurite.

In the literature, copper-based pigments are noted to be one of the types of pigments with which oxalate formation seems to be particularly pronounced (Higgitt and White 2005; Spring and Higgitt 2006; Salvadó et al. 2013). Zoppi et al. reported that calcium- and copper-containing pigments show the highest reactivity toward oxalic acid, due to their high solubility in an acid environment (Zoppi et al. 2010). In this case, however, analysis showed that although some copper oxalates were detected lower in the stratigraphy in certain green passages, the surface crusts only contain calcium oxalates. Examination of cross sections and UV-induced visible fluorescence imaging on the painting during cleaning showed that the crust was not directly adjacent to the original paint surface but separated from it by one or more varnish layers, strongly suggesting that its formation is unrelated to the degradation of the underlying paint. The heterogeneous composition of the crust, which contains

[14]For examples of the detection of calcium oxalate in easel painting, see Matteini et al. (2002), Higgitt and White (2005), Noble and Van Loon (2007), Van Loon (2008), Kahrim et al. (2009), and Salvadó et al. (2009, 2013).

compounds that are typical of airborne particles, suggests instead that its formation is linked to dirt deposition and that the calcium is primarily of atmospheric origin. Supporting this suggestion is the fact that the panels spent a long period in the Spanish monastery in Nájera where – more than in a museum environment – they are likely to have accumulated high levels of calcium-containing dust and been exposed to microbial action (Kontozova-Deutsch et al. 2011). The thickest crust formation was found over the dark-colored copper-containing paint layers. Such areas are likely to have been left untouched during past selective cleaning when varnish(es) might only have been removed from the light colors to obtain a quick result, allowing dirt to build up most over these passages. These conditions would favor the formation of calcium oxalate salts which have effectively "cemented" the dirt to the surface of the painting, creating the thick, highly insoluble, and disfiguring surface crusts. The presence of multiple layers of very discolored and dirty oil-resin varnish and overpaint below the crust in the dark paint passages further obscured the composition. The dark passages may also have benefitted from local varnishing to (re)saturate the colors, with such additional organic layers perhaps further enhancing the oxalate formation, in a similar way as suggested by some authors for stone monuments (Lazzarini and Salvadori 1989; Rampazzi et al. 2004).

15.7 Removal

As the thick crusts concealed every hint of color and every pictorial detail over large areas, they were very disturbing, reducing the artistic quality and legibility of the paintings. To be able to fully appreciate again the original quality of the paintings, their removal was an essential part of the ongoing cleaning of the panels. The varnish layers in between the crust and the original paint indicated that the crusts were not part of the original paint stratigraphy. Together with the international advisory committee that oversaw the conservation process, it was therefore decided to undertake this time-consuming operation.

The presence of an intermediate varnish layer made it possible to separate the crusts from the original paint surfaces. In the green areas, where solvents might damage the vulnerable glazes, this could only be done mechanically, with a scalpel under the microscope. Working under magnification and progressing only millimeter by millimeter, the conservators were able to remove the disfiguring crust. Time-consuming as it was, the results were spectacular as can be seen in Figs. 15.1 and 15.7. Underneath the dull, plain brown surface appeared lush green draperies with three-dimensional folds, brocade patterns in different green hues, and decorative details such as fringes applied using lead-tin-yellow, as predicted by the imaging techniques. In the UV-induced visible fluorescence photograph (Fig. 15.7), it can be seen that the fluorescent varnish layer located between the crust and the original paint surface was revealed after removal of the crust, again confirming the observations made from paint samples.

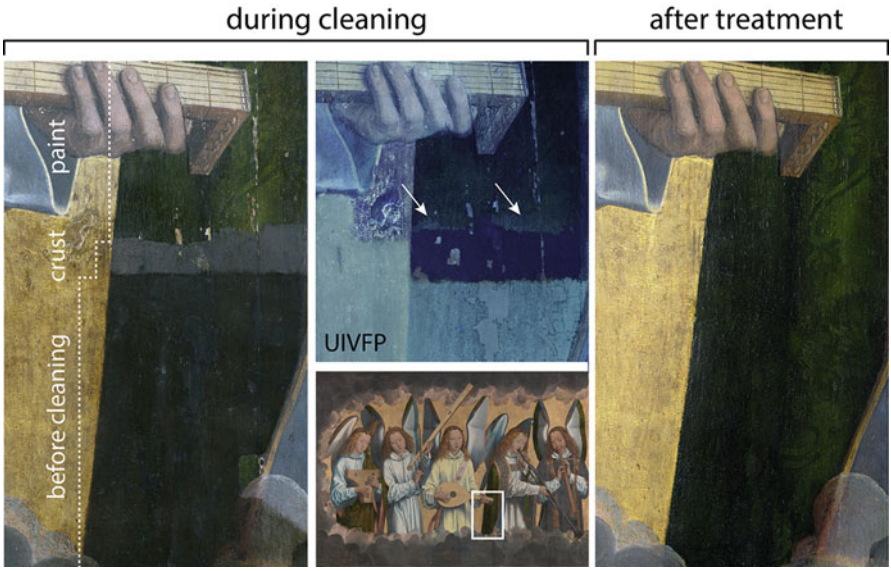

Fig. 15.7 Photo showing a detail of panel 779, as indicated by the white rectangle (middle, bottom). Left: cleaning staircase illustrating the gradual removal of the aged surface varnish(es) and the oxalate crust on the green paint. Middle, top: UV-induced visible fluorescence photograph (UIVFP) of the same area showing the typical fluorescence of the aged surface varnish(es) while the oxalate crusts appear dark in UV where exposed. Between the crust and the original paint surface, a fluorescent layer is visible (indicated by two white arrows), confirming the presence of an intermediate varnish layer. Right: the same area after treatment. Photo left: KMSKA © Arcobaleno, Adri verburg. Photo right: KMSKA © Rik Klein Gotink

Figure 15.8 illustrates how the gradual removal of the surface varnish layers and the underlying crust was documented in situ during the ongoing treatment by means of macroscopic FTIR scanning and spectroscopy in reflection mode.

The aim of these scans was to show the effectiveness of the (mechanical) cleaning procedure. As shown in the FTIR maps in Fig. 15.8, the distribution of the ν_s (CO) band of calcium oxalate clearly coincides with the crust, while the signal is absent where the green paint is revealed. The spectra in Fig. 15.8 were obtained in the latter cleaned area, proving what can be concluded from the oxalate distribution map: the intensity of the band at 1320 cm^{-1}, related to calcium oxalate, has dropped significantly after cleaning. Two paint losses appear as hot spots in the distribution maps for calcium carbonate, one of the materials employed in the preparation layers.

Although mechanical cleaning was possible on the smooth surface of the green colors, it was impossible on the more grainy blue colors and grey clouds. Removal of the crusts over the blue colors was possible to a certain degree by repeat applications of mixtures of dimethyl sulfoxide in ethyl acetate in different concentrations. On the grey clouds, a combination of solvent action and mechanical removal could be used. However, the vulnerability of the grey paint layer made it impossible to

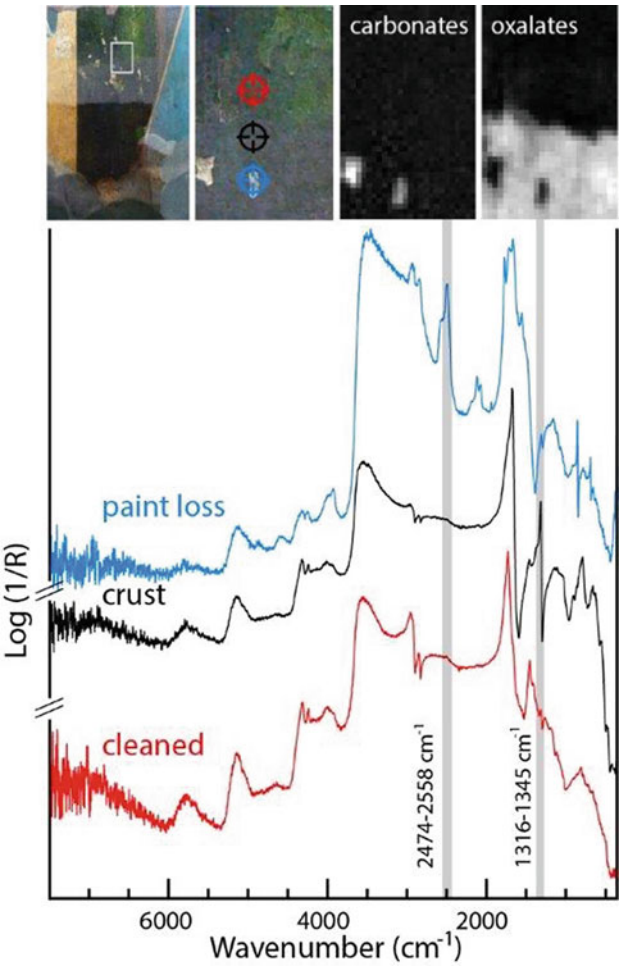

Fig. 15.8 Top, left: detail of the garment of angel 4 showing sequential cleaning tests. The white rectangle indicates an area where the crust was partially removed and imaged by means of macroscopic FTIR scanning in reflection mode. Top right: corresponding FTIR maps showing the distribution of carbonates in the paint losses and calcium oxalates in the crust. Bottom: FTIR spectra isolated from the hyperspectral data cube, with indication of the bands that were used to generate the chemical maps

remove the oxalate-containing crusts completely, and some material had to be left on the surface. Over the lighter colors, the oxalate-containing layers are very thin and hardly visible, for example, over the red feathers discussed above. In such areas, since the layers were not optically disturbing, they were left on the surface.

15.8 Conclusion

During the recent conservation of the three panels of Memling's *Christ with Singing and Music-making Angels,* an insoluble calcium oxalate-containing layer was found over the entire surface of the paintings. This crust was particularly thick, opaque, and disfiguring on the dark, copper-containing paint passages. The crust obscured the underlying composition but was extremely insoluble and posed a major conservation challenge.

A wide range of non-invasive and microinvasive analytical techniques were employed to determine the composition and distribution of the crusts and to establish the stratigraphy and nature of the underlying layers. Each contributed in a significant and complementary way to achieving as full an understanding as possible of the accretions on the paint surface, which was essential in informing the treatment of the paintings. The analytical results revealed that the crusts contained oxalate salts in the form of two related Ca-based oxalate salts, whewellite and weddellite, and a range of other components consistent with surface dirt deposition.

Oxalate salts have been found associated with a wide range of different artworks, and the mechanism of their formation is complex, possibly quite variable, and not fully understood. In the case of the Memling panels, the oxalates associated with the surface crusts did not appear to originate from degradation of the original paint but possibly from a combination of microbial action and a thick accumulation of dirt, particularly over the darker paint passages, where in addition a buildup of older varnishes had been left in place. The dirt deposits are likely to have accumulated during the period, while the panels were in the Nájera monastery.

The presence of intermediate varnish layer(s) between the crust and the original paint surface, as revealed by the analyses, indicated that the crusts were not part of the original paint stratigraphy and made it possible to remove most of them mechanically. The removal was a difficult and time-consuming process, and its progress was carefully monitored using macroscopic FTIR scanning and spectroscopy in the reflection mode. The treatment has, however, yielded spectacular results and has allowed the original colors and spatial depth of the composition to be recovered.

Acknowledgments A conservation project this large involves many people. Many thanks to Ineke Labarque, Régine Wittermann, Jean Albert Glatigny, Sara Matteu, Madeleine ter Kuile, Greta Toté, the advisory committee, and all colleagues from the conservation studio. We are indebted to the staff of the P06 beamline of the PETRA III facility and to DESY for providing the beam time for the synchrotron radiation-based measurements. KJ, GvdS, FV, and SL acknowledge financial support from the University of Antwerp Research Council via SOLARPAINT and other projects, the Fund Baillet Latour, and the Fund for Scientific Research (FWO), Brussels. CH and MS acknowledge the assistance of their colleague David Peggie. The conservation of the panels was supported by the Friends of the KMSKA and Interbuild NV, and the associated research was supported by the Baillet Latour fund.

References

Borchert T (1993) Memling's Antwerp "God the Father" with music-making angels. In: Verougstraete H, Van Schoute M (eds) Le dessin sous-jacent dans la peinture, Colloque X, September 1993, vol 1995. Le dessin sous-jacent dans le processus de creation, Louvain-la-Neuve, pp 153–168

Conti C, Brambilla L, Colombo C et al (2010) Stability and transformation mechanism of weddellite nanocrystals studied by X-ray diffraction and infrared spectroscopy. Phys Chem Chem Phys 12:14560–14566

De Nolf W, Janssens K (2010) Micro X-ray diffraction and fluorescence tomography for the study of multilayered automotive paints. Surf Interface Anal 42:411–418

De Nolf W, Vanmeert F, Janssens K (2014) XRDUA: crystalline phase distribution maps by two-dimensional scanning and tomographic (micro) X-ray power diffraction. J Appl Crystallogr 47:1107–1117

De Vos D (1994) Hans Memling. Het volledige oeuvre. Mercatorfonds, Antwerpen

Farmer V (1974) The layer silicates. In: Farmer V (ed) The infrared spectra of minerals. Mineralogical society monograph, vol 4. Mineralogical Society of Great Britain and Ireland, London, pp 331–363

Fransen B (2018) Hans Memling's Nájera altarpiece: new documentary evidence, The Burlington Magazine. Feb 2018. CLX 101–105

Garty J, Kunin P, Delarea J et al (2002) Calcium oxalate and sulphate-containing structures on the thallial surface of the lichen Ramalina lacera: response to polluted air and simulated acid rain. Plant Cell Environ 25:1591–1604

Gianoncelli A, Castaing J, Ortega L et al (2008) A portable instrument for *in situ* determination of the chemical and phase compositions of cultural heritage objects. X-Ray Spectrom 37:418–123

Gómara E (2013) Las tablas Najerinas del Muro de Amberes. Arte e Historia 21:16–19

Higgitt C, White R (2005) Analyses of paint media: new studies of Italian paintings of the fifteenth and sixteenth centuries. Natl Gallery Tech Bull 26:88–97

Janssens K, Legrand S, Van der Snickt G et al (2016) Virtual archaeology of altered paintings: multiscale chemical imaging tools. Elements 12:39–44

Kahrim K, Daveri A, Rocchi P et al (2009) The application of *in situ* mid FTIR fibre-optic reflectance spectroscopy and GC-MS analysis to monitor and evaluate painting cleaning. Spectrochim Acta A 74:1182–1188

Kontozova-Deutsch V, Cardell C, Urosevic M et al (2011) Characterization of indoor and outdoor atmospheric pollutants impacting architectural monuments: the case of San Jerónimo Monastery (Granada, Spain). Environ Earth Sci 63:1433–1445

Lazzarini L, Salvadori O (1989) A reassessement of the formation of the patina called 'scialbatura'. Stud Conserv 34:20–26

Legrand S, Alfeld M, Vanmeert F et al (2014) Macroscopic Fourier transform infrared scanning in reflection mode (MA-rFTIR), a new tool for chemical imaging of cultural heritage artefacts in the mid-infrared range. Analyst 139:2489–2498

Leroy C (2016) Oxalates de calcium et hydroxyapatite: des matériaux synthétiques et naturels étudiés par techniques RMN et DNP. PhD thesis in Chemistry, Université Pierre et Marie Curie, Paris. https://tel.archives-ouvertes.fr/tel-01443727. Accessed Feb 2017

Matteini M, Moles A, Lanterna G et al (2002) Characteristics of the materials and techniques. In: Ciatti M, Seidel M (eds) Giotto. The crucifix in Santa Maria Novella. Edifir, Florence, pp 387–403

Mendes N, Lofrumento C, Migliori A et al (2008) Micro-Raman and particle-induced X-ray emission spectroscopy for the study of pigments and degradation products present in 17th century coloured maps. J Raman Spectrosc 39:289–229

Miliani C, Rosi F, Sgamellotti A et al (2010) In situ noninvasive study of artworks: the MOLAB multitechnique approach. Acc Chem Res 43:728–738

Monico L, Rosi F, Miliani C et al (2013) Non-invasive identification of metal-oxalate complexes on polychrome artwork surfaces In reflection mid-infrared spectroscopy. Spectrochim Acta A 116:270–280

Noble P, Van Loon A (2007) Rembrandt's Simeon's song of praise, 1631: pictorial devices in the service of spatial illusion. Art Matters 4:19–35

Potgieter-Vermaak S, Godoia R, Van Grieken R et al (2005) Micro-structural characterization of black-crust and laser cleaning of building stones by micro-Raman and SEM techniques. Spectrochim Acta A 61:2460–2467

Rampazzi L, Andreotti A, Bonaduce I et al (2004) Analytical investigation of calcium oxalate films on marble monuments. Talanta 63:967–977

Salvadó N, Butí S, Nicholson J et al (2009) Identification of reaction compounds in micrometric layers from gothic paintings using combined SR-XRD and SR-FTIR. Talanta 79:419–428

Salvadó N, Butí S, Cotte M et al (2013) Shades of green in 15th century paintings: combined microanalysis of the materials using synchrotron radiation XRD, FTIR and XRF. Appl Phys A 111:47–57

Solé V, Papillon E, Cotte M et al (2007) A multiplatform code for the analysis of energy-dispersive X-ray fluorescence spectra. Spectrochim Acta B 62:63–68

Spring M, Higgitt C (2006) Analyses reconsidered: the importance of the pigment content of paint in the interpretation of the results of examination of binding media. In: Nadolny J (ed) Medieval paintings in northern Europe: techniques, analysis, art history. Studies in commemoration of the 70th birthday of Unn Plahter. Archetype, London, pp 223–229

Van der Snickt G, Miliani C, Janssens K et al (2011) Material analyses of 'Christ with singing and music-making Angels', a late 15th-C panel painting attributed to Hans Memling and assistants: Part I. non-invasive *in situ* investigations. J Anal At Spectrom 26:2216–2229

Van der Snickt G, Janssens K, Dik J et al (2012) Combined use of synchrotron radiation based micro-X-ray fluorescence, micro-X-ray diffraction, micro-X-ray absorption near-edge, and micro-Fourier transform infrared Spectroscopies for revealing an alternative degradation pathway of the pigment cadmium yellow in a painting by Van Gogh. Anal Chem 84:10221–10228

Van Grieken R, Gysels K, Hoornaert S et al (2000) Characterization of individual aerosol particles for atmospheric and cultural heritage studies. Water Air Soil Pollut 123:215–228

Van Loon A (2008) Color changes and chemical reactivity in seventeenth-century oil paintings. Dissertation, University of Amsterdam. MOLART Reports, vol. 14

Vandenbroeck P (1985) Catalogus schilderijen 14e en 15e eeuw. Ministerie van de Vlaamse Gemeenschap/Koninklijk Museum voor Schone Kunsten, Antwerpen, pp 138–143

Zoppi A, Lofrumento C, Mendes N et al (2010) Metal oxalates in paints: A Raman investigation on the relative reactivities of different pigments to oxalic acid solutions. Anal Bioanal Chem 397:841–849